第 35 卷第 6 期
2016 年 12 月

红 外 与 毫 米 波 学 报
J. Infrared Millim. Waves

Vol. 35, No. 6
December, 2016

文章编号: 1001 - 9014(2016)06 - 0662 - 05 **DOI**: 10. 11972/j. issn. 1001 - 9014. 2016. 06. 005

Dark current simulation and verification of $In_{0.83}Ga_{0.17}As$ detector with superlattice electron barrier

LI Qing-Fa[1,2,3,4], LI Xue[1,2], TANG Heng-Jing[1,2], DENG Shuang-Yan[1,2],
CAO Gao-Qi[1,2,3], SHAO Xiu-Mei[1,2], GONG Hai-Mei[1,2]*

(1. State Key Laboratories of Transducer Technology, Shanghai Institute of Technical Physics,
Chinese Academy of Sciences, Shanghai 200083, China;
2. Key Laboratory of Infrared Imaging Materials and Detectors, Shanghai Institute of Technical Physics,
Chinese Academy of Sciences, Shanghai 200083, China;
3. University of Chinese Academy of Sciences, Beijing 100049, China;
4. School of Physical Science and Technology, Shanghai Tech University, Shanghai 201210, China)

Abstract: To obtain the dark current mechanism of $In_{0.83}Ga_{0.17}As$ detector, TCAD software was used to simulate its dark current property. The detectors include two structures with and without the super lattice (SL) electronic barrier in the InGaAs absorbed layer. At the same time, the detector has been fabricated to verify the simulation results. The results show that SL barrier can adjust the energy band structure and change the transport property of the carriers, and thus suppress the SRH recombination and decrease the dark current. Simulation results are in good agreement with experimental results. The influence of the location and periods of SL barrier on dark current was also simulated. The SL electronic barrier structure was optimized.

Key words: $In_{0.83}Ga_{0.17}As$ detector, super lattice(SL) electronic barrier, dark current, TCAD simulation
PACS: 85. 60. -q

含有超晶格电子势垒的 $In_{0.83}Ga_{0.17}As$ 探测器暗电流仿真和验证

李庆法[1,2,3,4], 李 雪[1,2], 唐恒敬[1,2], 邓双燕[1,2], 曹高奇[1,2,3], 邵秀梅[1,2], 龚海梅[1,2]*

(1. 中国科学院上海技术物理研究所 传感技术国家重点实验室,上海 200083;
2. 中国科学院上海技术物理研究所 红外成像材料和器件重点实验室,上海 200083;
3. 中国科学院大学,北京 100049;
4. 上海科技大学 物质科学与技术学院,上海 201210)

摘要:为了获得 $In_{0.83}Ga_{0.17}As$ 探测器的暗电流机制,采用了 TCAD 软件对吸收层中含有和不含有超晶格电子势垒的 p-i-n 结构探测器暗电流特性进行仿真,并开展了器件验证. 结果表明,超晶格势垒可以调整器件的能带结构,改变载流子传输特性,降低 SRH 复合,从而降低器件的暗电流,仿真结果与实验结果吻合. 在此基础上,分析了势垒位置和周期变化对暗电流的影响,提出了进一步降低器件暗电流的超晶格电子势垒优化结构.

关 键 词: $In_{0.83}Ga_{0.17}As$ 探测器;超晶格电子势垒;暗电流;TCAD 仿真

中图分类号: TN215 **文献标识码**: A

Received date: 2016- 03- 08, **revised date**: 2016- 09- 29 **收稿日期**: 2016- 03- 08, **修回日期**: 2016- 09- 29

Foundation items: Supported by the National Key Basic Research and Development Program of China (2012CB619200), National Natural Science Foundation of China (61205105, 61376052, 61475179)

Biography: LI Qing-Fa(1990-), male, Weifang China, Master, Research area focus on InGaAs IR detector. E-mail: lqf1192008@163.com

* **Corresponding author**: E-mail: hmgong@mail.sitp.ac.cn

Introduction

Short-wavelength infrared (SWIR) InGaAs detectors has been applied in various fields, such as astronomical observation, earth detection and machine vision[1-2]. Detectors of $In_{0.53}Ga_{0.47}As$ with lattice matched with InP has a 1.7 μm cut-off wavelength at room temperature. However, in the remote sensing field, 1-2.5 μm is much more important wavelength range, which requires indium composition to be increased to 0.83. The $In_{0.83}Ga_{0.17}As$ detector has more defects due to its mismatch to the InP substrate. Besides, some groups showed that InAs/GaSb super lattice (SL) can be used in the mid-wavelength and long-wavelength infrared detectors to decrease the dark current[3-4], and InAs/InGaAs was also used to decrease the dark current in the SWIR InGaAs detector[5]. The dark current of the $In_{0.83}Ga_{0.17}As$ detectors has been decreased to about 1 nA/cm^2 at low temperature[6-7]. However, few papers analyzed the dark current mechanism of the $In_{0.83}Ga_{0.17}As$ detector with and without SL. There are few reported works for simulating and optimizing the structure of the detectors.

In this paper, technology computer aided design (TCAD) software was used to simulate the dark current of the $In_{0.83}Ga_{0.17}As$ detector based on theoretical model. By TCAD, two kinds of structure detectors with and without SL in the absorbed layer were simulated. At the same time, the detectors were also fabricated. Its current-voltage curves were measured by the Agilent B1500A Semiconductor Device Analyzer at room temperature (RT) and low temperature (LT). In addition, further optimization was simulated for different locations and periods of SL barrier.

1 Dark current theory of $In_{0.83}Ga_{0.17}As$ detector

The dark current of p-i-n detectors includes several distinct mechanisms, diffusion, generation recombination, trap-assisted tunneling (TAT) effect and so on. At room temperature, the dark current is limited by the diffusion process[5]. When the temperature falls, generation recombination mechanism dominated the dark current. As for generation recombination, Shockley-Hall-Read (SRH) mechanism, instead of the Auger recombination, plays the main role at low reverse bias or zero-bias because the carriers concentration of depletion region is very low at low reverse bias or zero-bias. In addition, the TAT current is the important component at low temperature[8-9].

The main dark currents in the $In_{0.53}Ga_{0.47}As$/InP near-infrared detector are the diffusion current and SRH generation-recombination current at room temperature and low temperature[10], respectively. However, for the $In_{0.83}Ga_{0.17}As$ on the InP substrate, there are many defects caused by the lattice mismatch, and the defects form the trap levels in the $In_{0.83}Ga_{0.17}As$ absorption layer. TAT can occur depending on the trap levels. Therefore, TAT mechanism should be considered in the dark current model of $In_{0.83}Ga_{0.17}As$ SWIR detector[11-12]. And the $In_{0.83}Ga_{0.17}As$ SWIR detector works at low bias, so the main mechanism of the dark current should be diffuse current, SRH current and TAT current. The dark current model can be expressed as

$$I_{TOTAL} = I_{DIFF} + I_{SRH} + I_{TAT} \quad . \quad (1)$$

The dark current model of $In_{0.83}Ga_{0.17}As$ detector in Ref. [13] reveals that the main components are diffusion and SRH current mechanism at zero-bias and room temperature. When the temperature becomes lower, the SRH current is suppressed and the TAT current becomes dominant. It is because that the energy gap becomes narrow and the tunneling effect happens easily at low temperature.

For the SRH generation recombination[14-15],

$$R_{SRH} = \frac{N_T(pn - n_1^2)}{\tau_{p0}\left[n + n_i\exp\left(\frac{E_i - E_T}{kT}\right)\right] + \tau_{n0}\left[p + n_i\exp\left(\frac{E_T - E_i}{kT}\right)\right]} \quad , \quad (2)$$

where τ_{p0} is the minority carrier lifetime due to SRH processes and τ_{n0} is the lifetime of electrons; n_i and E_i are the intrinsic carrier concentration and intrinsic Fermi level; E_T and N_T are the trap level and defects trap concentrations, p and n are the hole and electron concentrations, respectively.

2 Results and discussion

There are two kinds of structure, S_1 and S_2, used for simulating the current-voltage property of the detector. This is typical p-i-n structure of the SWIR $In_{0.83}Ga_{0.17}As$ detector, and the insets of Figs. 1(a) and (b) show the structure of the detectors in the simulation. The thickness of the P^+-$In_{0.83}Al_{0.17}As$ layer is 530 nm with indium component 0.83, and the density of hole is 6×10^{18} cm^{-3}. The thickness of i-$In_{0.83}Ga_{0.17}As$ layer is 1 500 nm, and its density of electrons is 5×10^{16} cm^{-3}. The thickness of the N^+-$In_xAl_{1-x}As$ layer is about 1 900 nm, and the component of indium x varies from 0.52 to 0.87.

Figure 1(a) and (b) are the energy band diagrams of S_1 and S_2 structure. The SL is inserted into the $In_{0.83}Ga_{0.17}As$ absorbed layer to improve the performance. After inserting the SL in the InGaAs absorbed layer, the energy band has some changes. Figure 2(a) is the $In_{0.66}Ga_{0.34}As$/InAs super lattice structure. With the help of the TCAD, their energy band diagrams can be obtained, as shown in Fig. 2(b). It has the same ten periods of $In_{0.66}Ga_{0.34}As$/InAs with a thickness of 10 nm for each period. The $In_{0.66}Ga_{0.34}As$/InAs super lattice is a good choice. The lattice constant of $In_{0.66}Ga_{0.34}As$ is smaller than that of $In_{0.83}Ga_{0.17}As$, while the lattice constant of InAs is bigger than that of $In_{0.83}Ga_{0.17}As$. In the SL structure, both $In_{0.66}Ga_{0.34}As$ and InAs have the same thickness, so the $In_{0.66}Ga_{0.34}As$/InAs SL layers have strain-compensated effect on the $In_{0.83}Ga_{0.17}As$ absorbed layer. The epitaxial layer was grown by gas source molecular beam epitaxy (GSMBE). By inserting SL barrier, the quality of the $In_{0.83}Ga_{0.17}As$ layer becomes better[5,16].

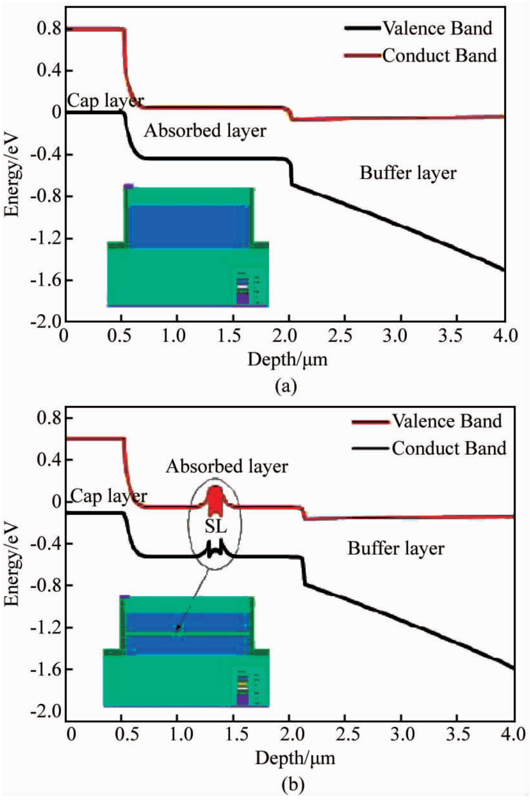

Fig. 1 Energy band of structure S_1(a) and structure S_2(b). The inserts illustrate the corresponding structures
图1 (a)S_1结构的能带图,(b)S_2结构的能带图;内插图是对应的结构

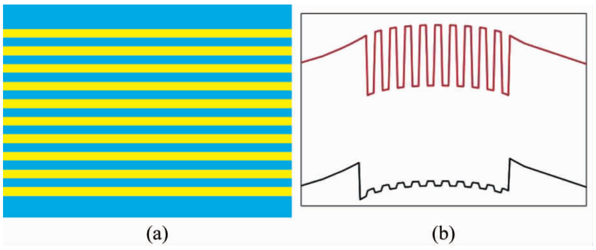

Fig. 2 (a) Super lattice barrier structure, (b) SL's energy band graph
图2 (a)超晶格势垒结构,(b)超晶格结构的能带图

Based on the S_1 and S_2 structures as shown in Fig. 1, two kinds of detectors, D_1 and D_2, were fabricated respectively, as shown in Fig. 3. In addition, the lattice constant of $In_{0.52}Al_{0.47}As$ matches to the InP substrate. The carrier concentration is about 4×10^{18} cm^{-3}. For the D_2, the thickness of the SL barrier in the middle of the absorbed layer is 0.1 μm. The simulation and experimental results of D_1 and D_2 are shown in Fig. 4. It is obvious that the dark current of D_2 decreases much than that of the traditional p-i-n structure detector D_1. The experimental and simulation results comply well at low bias, which verifies the feasibility of the TCAD model[17].

At room temperature, dark current at reverse bias is flat, which indicates that the current component mainly includes diffusion and SRH current. At -0.01 V, the experimental current density of D_1 is 8.27×10^{-4} A/cm^2 and simulation is 5.20×10^{-4} A/cm^2, while experimental current density of D_2 is 3.25×10^{-4} A/cm^2 and simulation is 1.87×10^{-4} A/cm^2, respectively. The current decreases to half of the original one after inserting the SL barrier. This is because that the barrier blocks the electrons recombinationin in the conduction band, that is to say the SRH recombination lifetime becomes longer so that the barrier can decrease the SRH current.

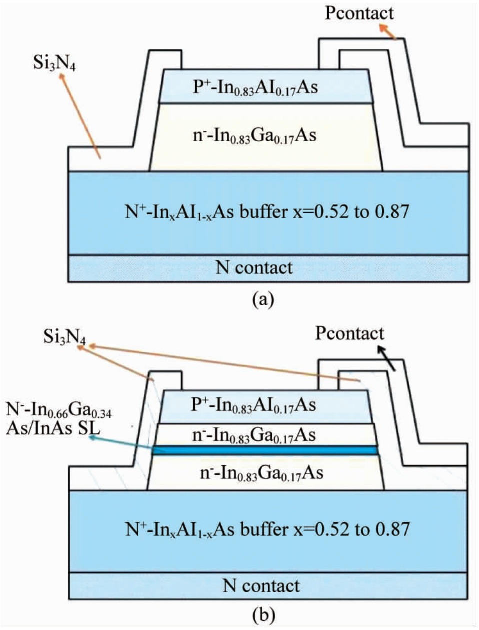

Fig. 3 (a) S_1 is the normal p-i-n structure, (b) S_2 is insertedSL electronic barrier in the absorbed layer
图3 (a)S_1结构是常规的p-i-n结构,(b)S_2结构是吸收层中插入超晶格电子势垒

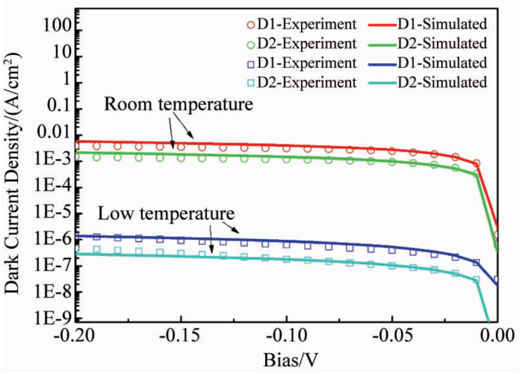

Fig. 4 *J-V* experiment and simulation curves of D_1 and D_2 at room temperature and low temperature
图4 器件D_1和D_2在室温和低温下的*J-V*实验和仿真拟合曲线

From the results of Fig. 4 at low temperature, it is obvious that the current components have been changed. At zero-bias, the dark current decreases larger than that at a relatively big revers bias. The reason is that the current has been dominant by the TAT current which is suppressed by the barrier at low temperature.

Table 1 Dark current density at -0.01 V under room temperature

表 1 室温下在-0.01 V 偏压的暗电流密度

Bias /V	D_1- Experiment	D_2- Experiment	D_1- Simulation	D_2- Simulation
Jd@ -0.01	8.27×10^{-4} A/cm^2	3.25×10^{-4} A/cm^2	5.20×10^{-4} A/cm^2	1.87×10^{-4} A/cm^2

Table 2 Dark current density at -0.01V under low temperature

表 2 低温下在-0.01V 偏压的暗电流密度

Bias /V	D_1- Experiment	D_2- Experiment	D_1- Simulation	D_2- Simulation
Jd @ -0.01	1.34×10^{-7} A/cm^2	2.98×10^{-8} A/cm^2	1.17×10^{-7} A/cm^2	2.55×10^{-8} A/cm^2

Above results proves that being inserted into the InGaAs absorbed layer, InAs/$In_{0.66}Ga_{0.34}As$ super lattice can decrease the dark current. Because the doping is the same, it formed the isotype heterojunction in their interface[18-19]. So its energy band graph has apparent changes. As shown in Fig. 2(b), conduction band has bigger barrier height than the valence band. This structure can change the carriers transport and form the electron barrier to block the electron in the conduction band. However, the hole carrier transport in the valence band. The barrier in the valence band is so small that the hole carrier can pass through barrier easily, so that the SL barrier has little effect for the photo response which depends on the hole carrier transport.

Location and period optimization of the electronic barrier was also studied. It is obvious that the SL barrier can adjust the energy band as shown in Fig. 2, so the location and period optimization should be taken into account.

We designed the simulation which used different distance from the location of the SL to interface between the cap layer and absorption layer, and named L_1, L_2, L_3. As shown in Table 3, L_1 is close to the depletion region, L_2 is close to the middle location of the absorbed layer and L_3 is close to the substrate. The simulation results are shown in Fig. 5(a). The results indicate that dark current first decreases and then increases with the increase of distance. The barrier can not only suppress the mismatch defects from the substrate, but also block the electron transporting to the depletion region for suppressing the electron current. When the location is on L_2, the interaction of two kinds can guarantee the dark current lower than that of L_1 and L_3. The thickness in one period was chosen as 5 nm, 10 nm, 15 nm or 20 nm. The results reveal that 15 nm is the better choice as shown in Fig. 5(b). When the period thickness is too thin, the barrier will be narrow and the tunneling will happen so that electrons can pass SL barrier. However the period is 15 nm, the barrier can block the electron current well. However the period is up to 20 nm, the barrier becomes wide so that the electrons can accumulate at the barrier well. Finally, the electric field enhancement can help the electron pass through the barrier.

Table 3 Different location of SL

表 3 超晶格的不同位置

	L_1	L_2	L_3
Location	1.1 μm	1.4 μm	1.6 μm

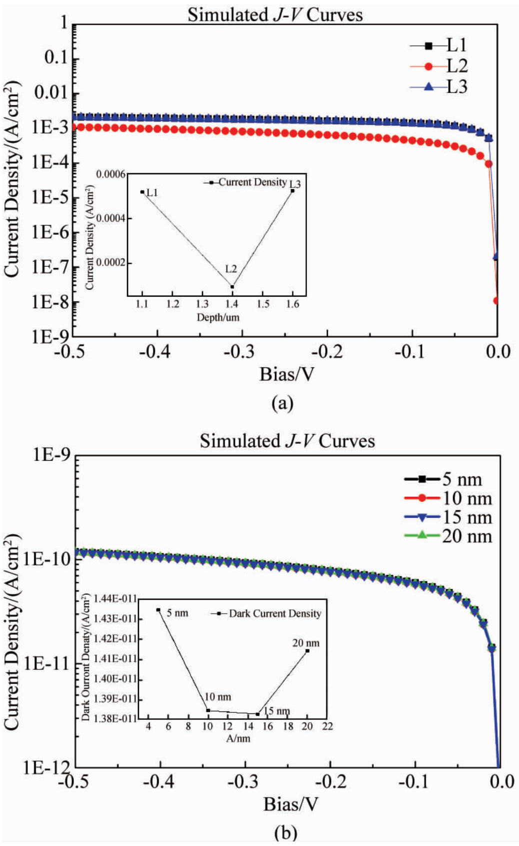

Fig. 5 *J-V* curves of different barrier locations and periods
图 5 超晶格势垒不同位置和周期的 *J-V* 曲线,内插图是在-0.01V 下的暗电流密度

3 Conclusion

In summary, we have studied dark current of $In_{0.83}Ga_{0.17}As$ detector with simulation and experimental method. It was found that the dark current can be suppressed effectively both at room temperature and low temperature by inserting $In_{0.66}Ga_{0.34}As$/InAs SL electronic barrier. In addition, the location and period of SL barrier can also affect the dark current. The dark current is low when the SL barrier with a period thickness of 15 nm is close to the middle location of the absorbed layer. The results are very useful for designing and obtaining detector with low dark current.

References

[1] Hoogeveen RW M, van der R J, Goede A P. Extended wavelength InGaAs infrared (1.0-2.4 μm) detector arrays on SCIAMACHY for space-based spectrometry of the Earth atmosphere[J]. *Infrared Physics & Technology*, 2001, **42**: 1-16.

[2] MacDougal M, Geske J, Wang C, *et al.* Low dark current InGaAs detector arrays for night vision and astronomy[J]. *Proceedings of SPIE*, 2009. **7298**: 72983F.

[3] Maimon S, Wicks G W. nBn detector, an infrared detector with reduced dark current and higher operating temperature[J]. *Applied Physics Letters*, 2006, **89**(15): 1109.

[4] Craig A P, Marshall A R J, Tian Z B, *et al.* Mid-infrared $InAs_{0.79}Sb_{0.21}$-based nBn photodetectors with $Al_{0.9}Ga_{0.2}As_{0.1}Sb_{0.9}$ barrier layers, and comparisons with $InAs_{0.87}Sb_{0.13}$ P-in diodes, both grown on

GaAs using interfacial misfit arrays[J]. *Applied Physics Letters*, 2013, **103**(25): 253502.

[5] Gu Y, Zhou L, Zhang YG, *et al*. Dark current suppression in metamorphic In$_{0.83}$Ga$_{0.17}$As photodetectors with In$_{0.66}$Ga$_{0.34}$As/InAs superlattice electron barrier[J]. *Applied Physics Express*, 2015, **8**(2): 022202.

[6] Gong H M, Shao X M, Li X, *et al*. Advanced technology and application of spaceborne infrared detectors[J]. *Infrared and Laser Engineering*, 2012, **41**:3129-3140.

[7] Gong H M, Li X, Li T, *et al*. Extended wavelength InGaAs infrared detector arrays based on three types of material structures grown by MBE[C]. Proceedings of SPIE, 2014, **9070**:90700C.

[8] Silvaco Inc. *ATLAS User's Manual*[M]. 2012.

[9] Ji X L, Liu B Q, Xu Y, *et al*. Deep-level traps induced dark currents in extended wavelength InxGa1-xAs/InP photodetector[J]. *Journal of Applied Physics*, 2013, **114**: 224502.

[10] Wang X D, Hu W D, Chen X S, *et al*. Dark current simulation of InP/In$_{0.53}$Ga$_{0.47}$As/InP p-i-n photodiode[J]. *Optical and Quantum Electronics*, 2008, **40**(14-15): 1261-1266.

[11] GU Y i, LI Cheng, WANG Kai, *et al*. Wavelength extended InGaAs/InP photodetector structure with lattice mismatch up to 2.6% [J]. *Journal of Infrared and Millimeter Waves*(顾溢,李成,王凯,等. 晶格失配度达2.6%的波长扩展InGaAs/InP光电探测器结构,**红外与毫米波学报**),2010, **29**(2):81-86.

[12] WEI Peng, HUANG Song-Lei, LI Xue, *et al*. Back illuminated InGaAs detector arrays with extended-wavelength to 2.4 μm[J]. Journal of Infrared and Millimeter Waves(魏鹏,黄松垒,李雪,等. 背照射波长延伸InGaAs面阵焦平面探测器,**红外与毫米波学报**)2013, **32**(3):214-219.

[13] Dwivedi A D D, Mittal A, Agrawal A, *et al*. Analytical modeling and ATLAS simulation of N$^+$-InP/n--In$_{0.53}$Ga$_{0.47}$As /p$^+$-In$_{0.53}$Ga$_{0.47}$As pin photodetector for optical fiber communication[J]. *Infrared Physics & Technology*, 2010, **53**(4):236-245.

[14] Ahrenkiel R, Keyes B, Dunlavy D. Intensity - dependent minority - carrier lifetime in III - V semiconductors due to saturation of recombination centers[J]. *Journal of Applied Physics*, 1991, **70**(1): 225-231.

[15] Ringel S A, Rohatgi A. The effects of trap-induced lifetime varitions on the design and performance of high-efficiency GaAs solar-cell[J]. *Electron Devices*, *IEEE Transactions on*, 1991, **38**(11): 2402-2409.

[16] Gu Y, Zhang YG, Liu S. Strain compensated AlInGaAs/InGaAs/InAs triangular quantum wells for lasing wavelength beyond 2 μm[J]. *Chinese Physics Letters*, 2007, **24**(11): 3237.

[17] Arslan Y, Oguz F, Besikci C. Extended short wavelength infrared In$_{0.83}$Ga$_{0.17}$As focal plane array[J]. *IEEE Journal of Quantum Electronics*, 2014, **50**(12):957-964.

[18] Kumar R. Current transport in isotype heterojunctions[J]. *International Journal of Electronics*, 1968, **25**(3): 239-247.

[19] Sun X, Li D, Li Z, *et al*. High spectral response of self-driven GaN-based detectors by controlling the contact barrier height[J]. *Scientific reports*, 2015, **5**: 16819.